Available online at www.sciencedirect.com
SCIENCE DIRECT®
Archives of Biochemistry and Biophysics 441 (2005) 84–95
ABB
www.elsevier.com/locate/yabbi

# A novel Arnt-interacting protein Ainp2 enhances the aryl hydrocarbon receptor signaling ☆

Yi Li, Tony C. Luu, William K. Chan *

*Department of Pharmaceutics and Medicinal Chemistry, Thomas J. Long School of Pharmacy and Health Sciences, University of the Pacific, Stockton, CA 95211, USA*

Received 31 March 2005, and in revised form 24 June 2005
Available online 27 July 2005

**Abstract**

In an effort to better understand the Ah receptor nuclear translocator (Arnt)-dependent signaling mechanisms, we employed a phage display system to identify Arnt-interacting peptides. Human liver cDNA library was utilized to screen for Arnt-interacting peptides using an Arnt construct fused to thioredoxin (TH-ArntCΔ418). Two clones, namely Ainp1 and Ainp2 (Arnt-interacting peptide), were identified and subsequently Ainp2 was further characterized. Ainp2 interacts with TH-ArntCΔ418 in the GST pull-down and mammalian two-hybrid assays. Northern blot results revealed that Ainp2 is predominantly expressed in human liver. The putative full-length Ainp2 cDNA sequence was subsequently cloned using RACE PCR. Endogenous expression of Ainp2 was found in Jurkat cells at the mRNA and protein levels. Results from the transient transfection studies using a DRE-driven reporter plasmid and the real-time QPCR experiments examining the endogenous CYP1A1 expression showed that Ainp2 enhances the 3-methylchloranthrene-induced activity in HepG2 cells, suggesting that Ainp2 plays a role in the Arnt-dependent function.


*Keywords:* AhR; Arnt; Arnt-interacting peptide; Phage display; Ainp; CYP1A1; AhR signaling

Ah receptor nuclear translocator (Arnt) is a basic-helix–loop–helix-PAS protein essential for the AhR[1] and HIF1α signaling. In the AhR signaling pathway, an AhR ligand triggers the nuclear translocation of the receptor, followed by the formation of the AhR-Arnt heterodimer which binds to the DRE, activates transcription of genes that encode drug metabolizing enzymes (such as CYP1A1 and 1A2) and other proteins (for review, see [1]). In response to hypoxia [2] or nitric oxide [3], the formation of the HIF-1α-Arnt heterodimer occurs which is followed by the transcriptional up-regulation of a battery of genes including VEGF, EPO, glucose transporters 1 and 3, and many glycolytic enzymes [4]. Studies on Arnt-null mice revealed that Arnt is essential for angiogenesis during embryonic development [5].

Phage display system has been effectively utilized to determine epitopes [6–8], isolate antibodies [9–11], and develop potential therapeutic agents [12–14] (for review, see [15]). Bacteriophage T7 can be used to express capsid fusion proteins with peptide cDNAs randomly cloned downstream to the capsid cDNA from a cDNA library; these fusion proteins are located on the phage surface. Phages containing the interacting peptides can then be preferentially precipitated by the bait protein. After

☆ Ainp2 GenBank accession number is DQ145726.

* Corresponding author. Fax: +1 209 946 2160.
*E-mail address:* wchan@pacific.edu (W.K. Chan).

[1] *Abbreviations used:* AhR, aryl hydrocarbon receptor; Arnt, Ah receptor nuclear translocator; HIF-1α, hypoxia inducible factor 1α; 3MC, 3-methylchloranthrene; βME, β-mercaptoethanol; TH-ArntCΔ418, thioredoxin-ArntCΔ418 fusion protein; TH-AhRCΔ553, thioredoxin-AhRCΔ553 fusion protein; GST, glutathione *S*-transferase; NBT, nitro-blue tetrazolium chloride; BCIP, 5-bromo-4-chloro-3-indolyl phosphate; SD, standard deviation Ainp2CTG, putative Ainp2 full-length cDNA with the start codon CTG; Ainp2DATG, same as Ainp2CTG except the start codon is mutated to ATG.

0003-9861/$ - see front matter © 2005 Elsevier Inc. All rights reserved.
doi:10.1016/j.abb.2005.06.026

several rounds of biopanning, interacting peptides can be enriched and then identified. For example, androgen receptor interacting peptides [16], 2-methylnorharman interacting peptides [17], EphA2 binding peptides SWL and YSA [18], Oct-4 interacting proteins [19], Glc7 as the HSF interacting protein [20], lipocalin-1 interacting membrane receptor [21] and Gal80p interacting proteins [22] have been discovered using this strategy.

It is our hypothesis that there are Arnt-interacting proteins that are essential for Arnt-dependent function (such as the AhR signaling) and are yet unidentified. For example, to activate gene transcription initiated by an AhR ligand, the AhR/Arnt/DRE ternary complex must form prior to the recruitment of coactivators to the promoter region. Our previous data showed that the formation of this ternary complex requires protein factors [23]. In other words, a number of unidentified proteins are necessary to cause the formation of the AhR/Arnt/DRE complex. We have shown that p23 [24] and CyP40 [25] potentiate the formation of the AhR/Arnt/DRE complex formation in vitro; however, the in vivo significance of these proteins is still unclear at present. Here, we report that we isolated an Arnt-interacting peptide Ainp2 using a phage display system. This Ainp2 is found in Jurkat cells and enhances the 3MC-mediated AhR signaling pathway.

## Materials and methods

### *Materials and reagents*

Human liver cDNA T7 phage library was purchased from Novagen (La Jolla, CA). pET-b expression vector for GST fusion protein synthesis was purchased from Novagen (La Jolla, CA). The mammalian two-hybrid kit was purchased from Promega (Madison, WI). The DRE-driven luciferase reporter plasmid pGudLuc1.1 was a gift from Dr. Mike Denison (UC, Davis). The β-galactosidase expressing plasmid pCH110 was purchased from Amersham–Pharmacia Biotech (Piscataway, NJ). *Escherichia coli* strains Top10 was purchased from Invitrogen (Carlsbad, CA) and BL21 (DE3) from Stratagene (La Jolla, CA). [$^{32}$P-γ]ATP and [$^{32}$P-α]ATP were purchased from MP Biomedicals (Irvine, CA). 3MC was purchased from Sigma (St. Louis, MO). Antiserum C634FB containing anti-Ainp2 polyclonal antibodies was obtained from chicken injected with the bacterially expressed antigen 6His-Ainp2CTG (Alpha Diagnostic, San Antonio, TX). The Anti-Thio antibody was purchased from Invitrogen (Carlsbad, CA). All PCR primers were purchased from Invitrogen (Carlsbad, CA). BugBuster and Cyto-Buster reagents were purchased from Novagen (La Jolla, CA). TALON metal resin was purchased from BD Biosciences (Palo Alto, CA). GST · BIND Resin was purchased from Novagen (La Jolla, CA). MEM media were purchased from Sigma (St. Louis, MO), cosmic calf serum from Fisher (Springfield, NJ), and all other cell culture reagents from Gibco (Carlsbad, CA). Lipofectamine 2000 was purchased from Invitrogen (Carlsbad, CA). Dual-Light luciferase and β-galactosidase reporter assay was purchased from Applied Biosystems (Tropix, Foster City, CA). MasterPure RNA Purification and FailSafe kits were purchased from Epicentre (Madison, WI). All Northern blot and RACE PCR related reagents were purchased from Ambion (Austin, TX). All other reagents, unless specified otherwise, were purchased from Fisher Scientific (Springfield, NJ).

### *Expression of thioredoxin fusion proteins (TH-ArntCΔ418 and TH-AhRCΔ553)*

The TH-ArntCΔ418 and TH-AhRCΔ553 proteins were expressed and purified according to previously published protocols with some modifications [26]. In brief, an 18-h LB culture (100 mL) containing the expression plasmid and ampicillin (50 μg/mL) was added to a fresh LB media (500 mL) containing ampicillin (50 μg/mL) and IPTG (1 mM final). Four hours induction at 37 °C, 250 rpm was allowed, followed by cell harvest. The cell pellet was resuspended in 45 mL lysis buffer (25 mM Hepes, pH 7.4, 300 mM NaCl, and 10% glycerol). Five milliliters of lysozyme solution (same buffer with 7.5 mg/mL of lysozyme) was added dropwise upon stirring. The suspension was stirred for 30 min, subjected to three freeze/thaw cycle times, and then followed by centrifugation at 16,000*g* for 30 min to obtain the supernatant. The supernatant was rocked with 0.25 mL of the pre-equilibrated TALON resin for 1 h before a column was poured. The resin was washed with 20 mL of purification buffer (25 mM Hepes, pH 7.4, 10% glycerol, and 300 mM NaCl), and then eluted with the same buffer in addition of 250 mM imidazole. The recombinant protein was eluted with the first 1.5 mL at a rate of 0.1 mL/min. After dialysis against 300 mL of 25 mM Hepes, pH 7.4, 10% glycerol, and 100 mM NaCl, the sample was stored at −80 °C.

### *TALON co-precipitation assay (biopanning)*

One microliter of the human cDNA T7 phage library or the amplified phage solution ($10^{10}$–$10^{11}$ pfu/mL) was precleared with the TALON resin (100 μL) in the assay buffer (800 μL, 25 mM Hepes, pH 7.4, 10% glycerol) by rotating the mixture at 32 rpm for 30 min at 4 °C. After brief centrifugation, the resin was discarded to remove nonspecific binding phages. The supernatant was then incubated with 100 μL TALON-purified of TH-ArntCΔ418 or an equal amount of thioredoxin as the negative control at 30 °C for 20 min before the addition of the TALON resin (100 μL) to the mixture. The mixture was rotated (32 rpm) at 4 °C for 5 h. After that, the

resin was washed 10 times with 0.9 mL of wash buffer (25 mM Hepes, pH 7.4, 10% glycerol, 250 mM KCl, 0.4% Tween 20, and 10 mM βME). The co-precipitated phages were then eluted with 0.3 mL of elution buffer (25 mM Hepes, pH 7.4, 250 mM imidazole). The eluted phages were subjected to titer determination and then enriched to a titer of $10^{10}$–$10^{11}$ pfu/mL via plate lysate amplification, ready for next round of biopanning.

*Membrane lift assay*

Phages were plated on a 100 mm LB agar plate to approximately 50–100 plaques. After the plaques grew to 0.5–1 mm in diameter, the plate was chilled at 4 °C for 30 min and then overlaid with a 82 mm nitrocellulose membrane at 4 °C for 1 min. The membrane was removed and blocked with 8 mL of blocking buffer (25 mM Hepes, pH 7.4, 10% glycerol, 100 mM KCl, and 10 mg/mL of nonfat dried milk) at 4 °C for 15 min. The membrane was then rotated with 6 mL of blocking buffer containing 10 μL of $^{32}$P-labelled TH-ArntCΔ418 [26] at 4 °C overnight at 32 rpm. After that, the membrane was washed three times with wash buffer (25 mM Hepes, pH 7.4, 10% glycerol, 100 mM KCl, 0.4% Tween 20, and 10 mM βME) and analyzed by autoradiography.

*Expression of GST-Ainp2 fusion proteins*

Ainp2 cDNA, either the phage peptide or the putative full-length sequence, was cloned into the *Bam*HI and *Hin*dIII sites of the pET-b vector. Expression of the GST fusion proteins (GST-Ainp2 and GST-Ainp2CTG) was performed as follows: IPTG induction (1 mM final) of 600 mL of LB culture was performed in BL21 (DE3) for 4 h at 37 °C, 250 rpm. The cells were lysed with 8 mL of BugBuster reagent and the supernatant, after centrifugation at 16,000*g* for 30 min, was applied onto a GST · BIND column (1 mL) at room temperature. The column was washed with 20 mL of purification buffer (25 mM Hepes, pH 7.4, 10% glycerol, and 100 mM NaCl) and then eluted with 3 mL of the same buffer except that GSH (10 mM) was included. After dialysis, the sample was then stored at −80 °C.

*GST pull-down assay*

A fixed amount (7.5 μg) of GST, GST-Ainp2, or GST-Ainp2CTG was incubated with 100 μL of TH-ArntCΔ418 in 1 mL of assay buffer (25 mM Hepes, pH 7.4, 10% glycerol) at 30 °C for 20 min. The sample solution was then rotated with 200 μL of the GST · BIND resin at 4 °C for 5 h at 32 rpm. After centrifugation at 16,000*g* for 45 s, the supernatant was discarded and the pellet was washed four times with wash buffer (25 mM Hepes, pH 7.4, 10% glycerol, 100 mM KCl, 0.4% Tween 20, 10 mM βME, and 5 mM imidazole) and then eluted with 100 μL of the SDS–PAGE sample buffer. The samples were subjected to 12% SDS–PAGE, followed by Western blot analysis using the Anti-Thio antibody and NBT/BCIP for signal detection, according to previously published protocols [24].

*Northern blot analysis*

Interestingly, a significant part of the cDNA sequence of Ainp2 is reverse complement to the haptoglobin cDNA. Thus, we made certain that only the antisense probe for Ainp2 was synthesized so that there is not a chance for the probe to hybridize with the haptoglobin mRNA. A 176-bp antisense cDNA fragment of Ainp2 was labeled with [$^{32}$P-α]dATP using the StripAble PCR probe synthesis kit with a single primer 5′-TGATAA GAGCTGTGCTGTGGCTGA-3′ and a linearized Ainp2 DNA sequence digested from pGEM-Ainp2 as the template. The $^{32}$P antisense cDNA probe was synthesized by PCR as follows: 30 s at 94 °C, 30 s at 50 °C, and 30 s at 72 °C, 50 cycles. The pre-made blot was first prehybridized with 7 mL of Ultrahyb buffer at 42 °C for 30 min and then incubated with the $^{32}$P antisense cDNA probe at a concentration of $10^6$ cpm/mL at 42 °C for 21 h, followed by two washes with NorthernMax high stringency wash buffer (2× SSC, 0.1% SDS) at 42 °C for 5 min and one wash with NorthernMax low stringency wash buffer (0.1× SSC, 0.1% SDS) at 4 °C for 15 min. The pre-made blot was stripped using StripAble PCR probe removal kit and reprobed with $^{32}$P-β-actin probe synthesized accordingly (template, Ambion PTRIampl8; primer, Ambion T7 primer; PCR protocol, 30 s at 94 °C, 30 s at 55 °C, and 1 min at 72 °C, 50 cycles) for normalization.

*RACE PCR*

FirstChoice PCR-ready human liver cDNA was used to perform the 5′ and 3′ RACE PCR to amplify the full-length cDNA sequence of Ainp2. For 5′ RACE, the antisense Ainp2 primer (OL127, nt 217–242) and the 5′ adaptor primer was used whereas for 3′ RACE, the sense Ainp2 primer (OL126, nt 77–99) and the 3′ adaptor primer was used. The PCR protocol was as follows: 30 s at 94 °C, 30 s at 60 °C, and 1.5 min at 72 °C, 35 cycles. The amplified products were subsequently cloned, purified, and sequenced.

*RT-PCR and Western blot analysis to detect Ainp2 expression*

Human lymphoid cell line Jurkat were grown in RPMI1640 supplemented with 10 mM HEPES (pH 7.25), 10% FBS, 0.2 mM L-glutamate, 100 U/mL penicillin, and 0.1 mg/mL streptomycin. HepG2 and Hepa-1 cells were grown in Advanced MEM supplemented with

5% cosmic calf serum, 0.2 mM L-glutamate, 100 U/mL of penicillin, and 0.1 mg/mL streptomycin. Upon harvest, cells were subjected to either RNA extraction using the MasterPure RNA purification kit or protein extraction using CytoBuster reagent. For protein extraction, enough CytoBuster reagent (50 μL per 18 mg of cell pellet) was added to each sample and then the samples were incubated for 10 min at room temperature. After that, freeze/thaw cycle was performed three times before sample centrifugation (16,000*g*, 10 min, 4 °C) to obtain the soluble extract. RT-PCR was performed to detect the Ainp2 mRNA as follows: first strand cDNA was synthesized using 1 μg of total RNA (from cells or rat liver) and random primers according to the Epicentre's protocol. One microliter of the reverse transcription reaction mixture was used as the template for the following PCR with the Ainp2 specific primers (sense (OL124), 5′-ATCCACTCCTGTCCACTCCCGTCC-3′ and antisense (OL143), 5′-AGGCAGGGTGTTGGCTTTAC-3′): 30 s at 94 °C, 30 s at 50 °C, and 1.5 min at 72 °C, 35 cycles. For Western blot analysis, proteins of the soluble extract was separated on a 15% tricine SDS–PAGE gel and antiserum C634FB (1:500) was used as the primary antibodies. Colorimetric assay using NBT/BCIP was performed to detect the signals. To co-precipitate the anti-Ainp2 antibodies from the antiserum C634FB, 0.6 μL of C634FB was incubated with 20 μL of the bacterially expressed 6His-Ainp2CTG (8 μg), 140 μL PBS, 140 μL of non-fat dried milk in PBS (50 mg/mL, 0.2% Tween 20) and 100 μL of the TALON resin for 2 h at room temperature. After incubation, the mixture was centrifuged at 16,000*g* for 10 min at 4 °C and the supernatant was then used as the primary antibodies.

*Mammalian two-hybrid assay*

The ArntCΔ418 cDNA was cloned into the *Bam*HI and *Xba*I sites of the pACT vector containing the cDNA of the VP16 transactivation domain. Additionally, the Ainp2 peptide cDNA were cloned into the *Bam*HI and *Xba*I sites of the pBIND vector containing the cDNA of the GAL4 DNA binding domain. HepG2 cells were grown to 80% confluence in a 24-well plate in Advanced MEM supplemented with cosmic calf serum (5%), L-glutamate (0.2 mM), penicillin (100 U/mL), and streptomycin (0.1 mg/mL). A transfection mixture of 200 μL of OPTI-MEM I medium containing plasmids (0.2 μg each of the pACT-ArntCΔ418, pBIND-Ainp2, PG5luc and pCH110 vectors) and 2 μL of Lipofectamine 2000 was added to each well, followed by incubation at 37 °C for 5 h. The media were then replaced with the complete media. After incubation at 37 °C for 24 h, cells were harvested for luciferase assay as follows: the cells were immediately lysed by the addition of 200 μL/well of the lysis buffer (100 mM potassium phosphate, pH 7.4, 1% Triton-X100, and 0.5 mM DTT) and rotation at 150 rpm for 10 min at room temperature, followed by centrifugation at 16,000*g* for 2 min. The supernatants (10 μL) were subjected for luciferase and β-galactosidase assays using the Dual-Light Kit, according to manufacturer's recommendation, using a Turner Design TD-20/20 luminometer. All transfection experiments were performed in triplicates and all the luciferase activities were normalized by the internal β-galactosidase activity.

*Transient transfection/luciferase assay*

HepG2 cells were grown to 80% confluence in a 24-well plate. A transfection mixture of 200 μL of OPTI-MEM I media containing plasmids (0.33 μg each of pGudLuc1.1, pCH110, pCMV-Tag4 or pCMV-Ainp2CTG or pCMV-Ainp2ΔATG) and 2 μL of Lipofectamine 2000 was added to each well, followed by incubation at 37 °C for 5 h. Complete media was exchanged and after 18 h at 37 °C, the cells were treated with either 1 μM 3MC or DMSO for 5 h at 37 °C before harvest. Luciferase assay was performed as described in the above session. We used MCF7 cells to examine the mammalian expression of 6His-Ainp2CTG protein by transient transfection studies. MCF-7 cells were grown in Advanced DMEM/F12 supplemented with 5% FBS, 0.2 mM L-glutamate, 100 U/mL penicillin, and 0.1 mg/mL streptomycin to 80% confluence in a six-well plate. Each well was transfected with 3 μg of pCMV-6His-Ainp2CTG plasmid, 6 μL of Lipofectamine 2000 in 0.5 mL of OPTI-MEM I media. Five hours after transfection, fresh complete media were exchanged, followed by a 24-h incubation at 37 °C before harvest. Cytobuster reagent was used to prepare the soluble extracts.

*Transient transfection/RT/real-time QPCR*

HepG2 cells were grown to 80% confluence in a 6-well plate. A transfection mixture of 500 μL of OPTI-MEM I media containing plasmids (3 μg each of pCMV-GST or pCMV-GST-Ainp2CTG) and 6 μL of Lipofectamine 2000 was added to each well and the cells were incubated at 37 °C for 5 h. Complete MEM was exchanged and incubation was allowed for 18 h at 37 °C. Then, the cells were treated at 37 °C with 1 μM 3-MC or DMSO for 5 h. After induction, the cells were immediately lysed and total RNA was prepared using the MasterPure RNA purification kit. RT/real-time PCR was performed using the FailSafe kit (with SYBR Green I dye) and a DNA Engine Opticon 2 System (MJ Research). The first cDNA strand was synthesized at 37 °C for 60 min using random primers. Subsequent PCR using 1A1 or 18S specific primers [1A1 sense (OL109): 5′-GGCCACATCC GGGACATCACAGA-3′; 1A1 antisense (OL110): 5′-TGGGGATGGTGAAGGG GACGAA-3′; 18S sense (OL96): 5′-CGCCCCCTCGAT GCTCTTAG-3′; 18S antisense (OL97): 5′-CGGCGGGT CATGGGAATAAC-3′] was performed as follows:

CYP1A1/18S—30 s at 94 °C, 30 s at 55 °C, and 45 s at 70 °C. Typically we set the run to 30 cycles. The final PCR products were analyzed by agarose gel electrophoresis. Relative abundance was determined by the cycle threshold ($C_T$) according to the equation and normalized by the 18S standard.

## Results

### *Biopanning and membrane lift assay to enrich Arnt-interacting phages*

We employed the TALON co-precipitation assay as the biopanning protocol to screen for Arnt-interacting proteins, followed by the membrane lift assay to confirm the interaction (Scheme 1). To try out this strategy, we want to use an Arnt bait that can be obtained quickly and abundantly. From our experience, one of the best ways to quickly express soluble recombinant proteins in an abundant amount is to express them as thioredoxin fusion proteins in bacteria with a size smaller than 60 kDa [26]. For this reason, we designed the bait as an Arnt construct CΔ418 (aa 1–371), lacking 418 amino acids from the C-terminus, fused to the C-terminus of thioredoxin to form TH-ArntCΔ418 (Fig. 1). To be certain that the Arnt moiety of TH-ArntCΔ418 was folded properly, we examined the interaction between this construct and AhRCΔ553 (lacking 553 amino acids from the AhR C-terminus) in the TALON co-precipitation assay. The silver stain results showed that AhRCΔ553 was co-precipitated as expected (Fig. 2A). Thioredoxin and TH-ArntCΔ418 were expressed and purified adequately for the biopanning protocol (Fig. 2B). After five rounds of biopanning, the phage titer was enriched to more than 100-fold (from 8 to 800 plaques) whereas the negative control, of which thioredoxin instead of TH-ArntCΔ418 was used as the bait, gave only 15-fold (from 2 to 30 plaques) enrichment (Figs. 2C and D). The enriched phages were then amplified and screened by the membrane lift assay to confirm that the phages indeed interacted with Arnt. Results from the membrane lift assay showed that 87% of the plaques (26 out of 30 plaques screened) interacted with $^{32}$P-THArntCΔ418 (data not shown). Among the 26 positive plaques, 24 of them were extracted and subjected for PCR to determine the sizes of the unknown cDNA (the remaining two were lost during the extraction). The PCR results showed that six of them were 600 bp, four 500 bp, eleven 300 bp, and two 200 bp (Fig. 2E). One plaque gave two products of 300 and 600bp which was most likely caused by contamination during sample preparation. Out of these 24 cDNA fragments, we performed restriction digest on ones with 300 and 600 bp using *Hae*III and *Sac*II. Five of the six 600 bp fragments were identical; we named them as Ainp1. Five of the eleven 300 bp fragments were identical and named as Ainp2. The Ainp2 peptide contains 58 amino acids (176 bp). The putative full-length

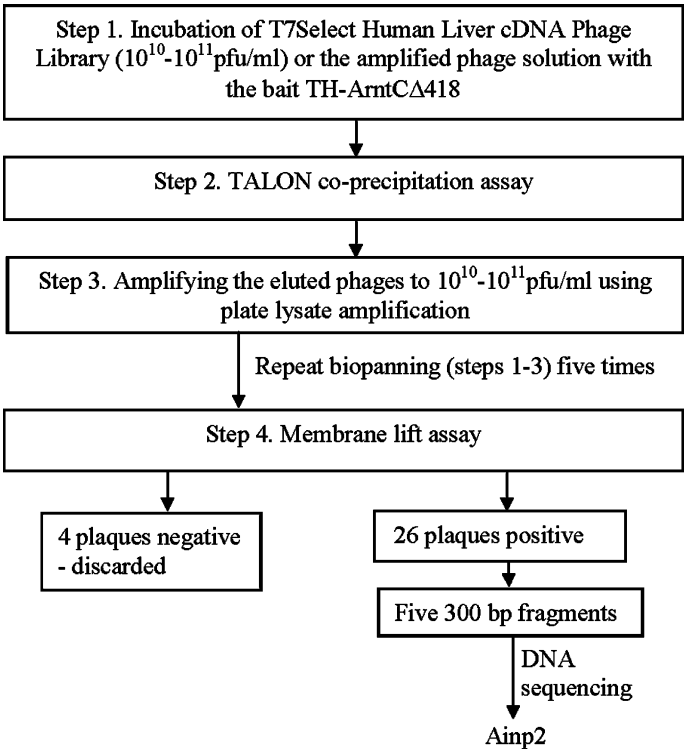


Scheme 1. Flowchart of the phage display system using T7Select human liver cDNA library.

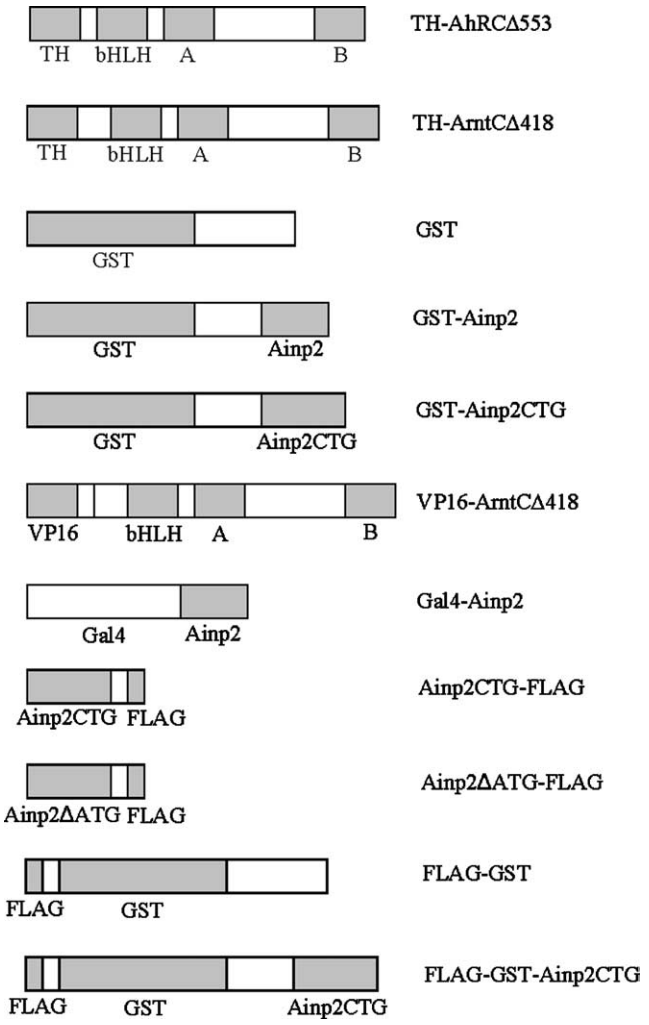


Fig. 1. Domain map of recombinant proteins made for this study.

cDNA of Ainp2 (Ainp2CTG) was subsequently cloned by RACE PCR and shown to contain 77 amino acids (Fig. 3).

Another unique 600 bp cDNA, which we called Ainp3 and has an open reading frame of 87 nucleotides, is not discussed in this paper. The remaining six 300 bp fragments were different from one another and were not pursued further. We did not analyze the 500 bp fragments because we were not able to recover the phage DNA after amplification for unknown reasons; the 200 bp fragments were not analyzed as well due to their small sizes.

*In vitro interaction between Arnt and Ainp2*

To examine whether Ainp2 interacts with Arnt, GST fusion proteins containing Ainp2 peptide or its putative full-length sequence were expressed in XLI-Blue (Figs. 1 and 4A, top) for GST pull-down assay. GST-Ainp2 or GST-Ainp2CTG was used as the bait and GST as the negative control. The results showed that in the presence of GST-Ainp2 and GST-Ainp2CTG, 4.8 and 4.3% of the amount of TH-ArntCΔ418 used for the assay were co-precipitated, respectively, whereas undetectable amount of TH-ArntCΔ418 was co-precipitated in the presence of the GST control (Fig. 4B), showing that both Ainp2 and Ainp2CTG interact with Arnt to a similar extent in vitro. We realized that our GST-Ainp2CTG contains intense lower bands that are also found in GST alone (Fig. 4A, bottom). When we normalized the amount of the lower bands of GST-Ainp2CTG and GST and used them as baits for the GST pull-down assay, only GST-Ainp2CTG co-precipitated TH-ArntCΔ418, supporting that Ainp2CTG, but not the lower bands, interacts with Arnt (data not shown).

*Interaction between Arnt and Ainp2 within intact cells*

To confirm that Ainp2 is capable of interacting with Arnt intact cells, mammalian two-hybrid studies were performed. Ainp2 was fused with the Gal4 DBD whereas ArntCΔ418 was fused with the transactivation domain VP16. An UAS-driven luciferase reporter plasmid was used. It is known that MyoD interacts with id; thus, plasmids expressing Myo-D and id are provided with the kit as positive controls. We used them as the negative controls by pairing MyoD with Ainp2 and id with ArntCΔ 418 because they should not interact. The transfection data showed that Gal4-Ainp2 increased the luciferase activity by 6.6-fold when compared to the negative controls (Fig. 5), supporting that Ainp2 interacts with Arnt intact cells.

*Endogenous expression of Ainp2 in human liver and Jurkat cells*

To confirm that Ainp2 is an endogenous protein, expression of the Ainp2 mRNA and protein was examined. Results from the Northern blot using a human pre-made blot showed that the Ainp2 mRNA is predominantly found in human liver but not in brain, placenta, skeletal muscle, heart, kidney, pancreas, lung, spleen, and colon (Fig. 6). However, when we examined the expression of Ainp2 in hepatoma cell lines HepG2 and Hepa-1, no Ainp2 expression was found (Fig. 7A). In addition, we did not observe Ainp2 protein expression in cryopreserved human hepatocytes (BD Biosciences). From a sequence search in GenBank using the Ainp2 cDNA (nt 1–1071) that we obtained from our RACE PCR, we found eight EST clones (BX448994, BX448865, BX427152, BX367157, BX367037, BX325183, AL579899, and AL563931) from Jurkat cells that have a complete match to our Ainp2 open reading frame (nt 117–350). In comparison, our Ainp2 cDNA has unique sequences at the very 5′ (nt 1–45) and 3′ (nt 876–1071) ends. Additionally, the Ainp2 cDNA is the reverse complement to the haptoglobin cDNA, with the same regions of Ainp2 cDNA (nt 1–45 and 877–1071) that are

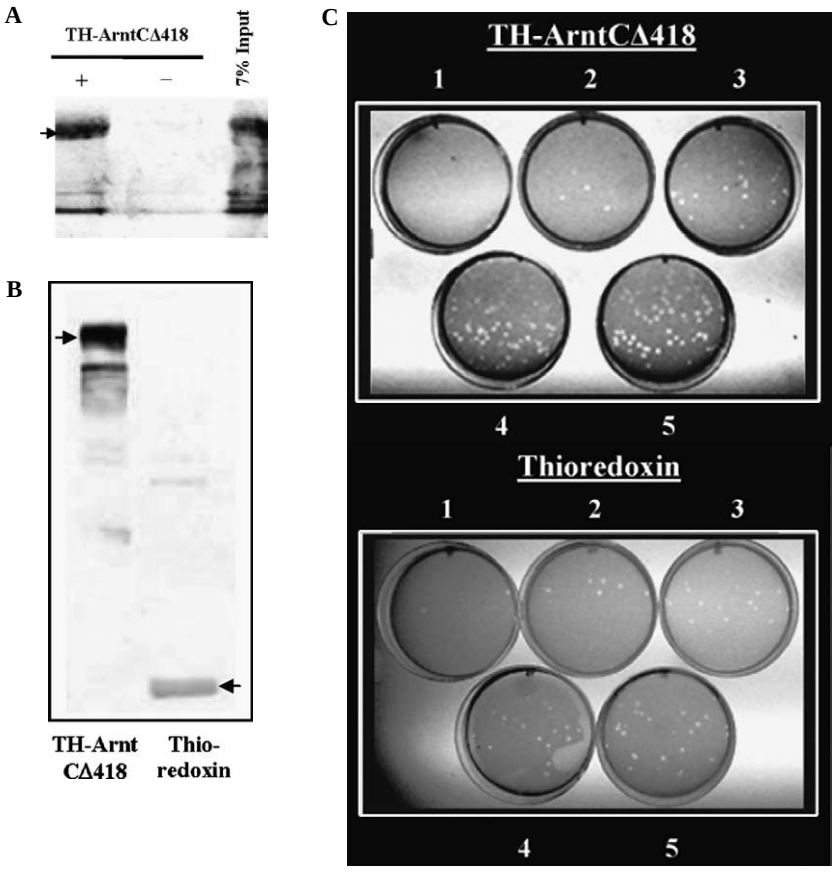


D

| Bait (below)/ Round of biopanning (right) | 1 | 2 | 3 | 4 | 5 |
|---|---|---|---|---|---|
| TH-ArntCΔ418 ($10^3$ pfu/ml) | 8 | 80 | 250 | 700 | 800 |
| Thioredoxin ($10^3$ pfu/ml) | 2 | 10 | 20 | 25 | 30 |

E

| cDNA insert size (bp) | Plaque No. | Number of plaques |
|---|---|---|
| 600 | 4,16,18,19,22,24 | 6 |
| 500 | 13,17,21,23 | 4 |
| 300 | 1,2,5,7,8,9,10,11,12,14,15 | 11 |
| 200 | 3,6 | 2 |
| 300/600 | 20 | 1 |

Fig. 2. Phage display revealing Arnt-interacting phages. (A) Silver staining of a 12% polyacrylamide gel showing the result using TH-ArntCΔ418 as the bait and the TALON resin to coprecipitate AhRCΔ553. Lane 1, TH-ArntCΔ418, 100 μL; lane 2, no TH-ArntCΔ418; lane 3, 7% of the amount of AhRCΔ553 used for the assay (input). The arrow indicates AhRCΔ553. (B) Western blot of TH-ArntCΔ418 and thioredoxin. Samples were separated by a 15% SDS–PAGE gel, followed by Western blot analysis using mouse Anti-Thio monoclonal antibody. NBT/BCIP was used to visualize the bands. The arrows indicate TH-ArntCΔ418 (56 kDa) and thioredoxin (11 kDa). (C) Plate assay using phages after each round of biopanning. Serial dilution of phages according to the phage titers determined by plate lysate amplification (1:1000 for TH-ArntCΔ418 and 1:100 for thioredoxin). The numbers represent the round of biopanning. Thioredoxin was used as the negative control. (D) Table showing the quantification of the results shown in (C). For TH-ArntCΔ418, the titer increased by 100-fold after five rounds of biopanning (from 8 to $800 \times 10^3$ pfu/mL) whereas for thioredoxin, the titer increased by 15-fold (from 2 to $30 \times 10^3$ pfu/mL). (E) Table showing the cDNA of positive clones from membrane lift. Twenty-four plaques which showed positive images on membrane lift were analyzed by PCR using the specific T7SelectUP and T7SelectDOWN primers (Novagen, La Jolla, CA). The amplified cDNA inserts were analyzed using a 1.5% agarose gel and categorized into five groups according to their sizes.

unique in comparison. With this information, we designed a primer set of Ainp2 (nt 75–98 and 976–995) that should only amplify the Ainp2 cDNA in Jurkat cells. Results from the RT-PCR experiment showed that Ainp2 transcript is present in Jurkat cells (Fig. 7A, upper). This PCR product has been purified and sequenced to confirm that it is indeed Ainp2. In addition, we used the crude serum C634FB containing the Ainp2 specific antibodies to perform Western blot analysis of the Jurkat cell extracts. Although this analysis revealed

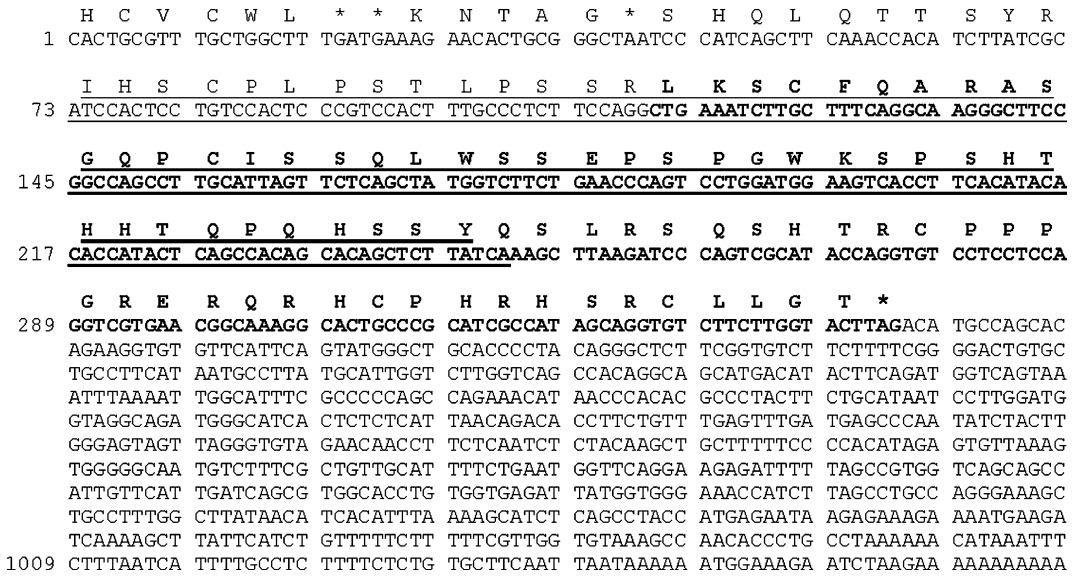


Fig. 3. Nucleotide and amino acid sequences of Ainp2. The Ainp2 peptide (underlined) and the putative full-length (bold) sequences are shown. The * indicates the in-frame stop codons at the 3′ and 5′ UTR.

that multiple bands could be detected when using the crude serum, a band of approximately 20 kDa disappeared when the serum was pre-treated with 6His-Ainp2CTG to co-precipitate the anti-Ainp2 antibodies from the serum using the TALON resin (Fig. 7B), supporting the idea that this 20 kDa protein is the endogenous Ainp2 (Fig. 7A, lower).

*Effect of Ainp2 on the luciferase activity up-regulated by 3MC in HepG2 cells*

To examine whether Ainp2 affects the AhR signaling, we performed transient transfection experiments using a luciferase reporter plasmid regulated by the mouse CYP1A1 promoter. The putative Ainp2 full-length cDNA with its CTG start codon (Ainp2CTG) or a mutated ATG (Ainp2ΔATG) was expressed under the control of the CMV promoter and the pCMV-Tag2 empty plasmid was used as the negative control. Induction of the luciferase activity by 3MC was increased from 2.6-fold to 6.2- and 6.8-fold in the presence of Ainp2CΔATG and Ainp2CTG, respectively. In addition, both Ainp2CTG (1.7-fold ± 0.06) and Ainp2ΔATG (1.8-fold ± 0.23) caused a statistically significant increase in the 3MC-induced luciferase activity over the empty vector (Fig. 8). These results suggested that Ainp2 may play a role in the gene regulation mediated by AhR.

*Effect of Ainp2 on the CYP1A1 induction by 3MC in HepG2 cells*

To examine whether Ainp2 affects the endogenous gene regulation mediated by AhR, we induced CYP1A1 mRNA level by 3MC in HepG2 cells in the presence of GST-Ainp2CTG or GST. We performed RT/real-time QPCR to quantify the CYP1A1 message. The results showed that induction of the CYP1A1 message by 3MC was enhanced at least 1.5-fold by GST-Ainp2CTG over the GST control (Fig. 9), supporting that Ainp2 may play a role in the AhR signaling. The amount of GST and GST-Ainp2CTG expressed in HepG2 cells was about the same, according to our RT-PCR results (data not shown).

*Expression of 6His-Ainp2CTG in Sf9 and MCF7 cells*

To examine whether Ainp2 is post-translationally modified in eukaryotic cells, we utilized the baculovirus system to overexpress 6His-Ainp2CTG in Sf9 cells using the BaculoGold kit (PharMingen) [23]. In addition, we expressed 6His-Ainp2CTG in MCF7 cells by transient transfection. After affinity purification using the TALON resin, we obtained most of the baculovirus 6His-Ainp2CTG that has the same size as the bacterially expressed protein. Interestingly, a small fraction of 6His-Ainp2CTG in Sf9 cells has a higher molecular weight (Fig. 10, lane 3), suggesting that it has been modified post-translationally. Expression of 6His-Ainp2CTG in MCF7 cells showed two bands: the minor (bottom) band has the same size as the bacterially expressed protein whereas the major (top) band appears to be post-translationally modified (Fig. 10, lane 6). These two bands are absent in the wild type MCF7 cells (Fig. 10, lane 7). Expression of 6His-Ainp2CTG protein in Sf9 and MCF7 cells is consistent with our prediction that Ainp2 is post-translationally modified.

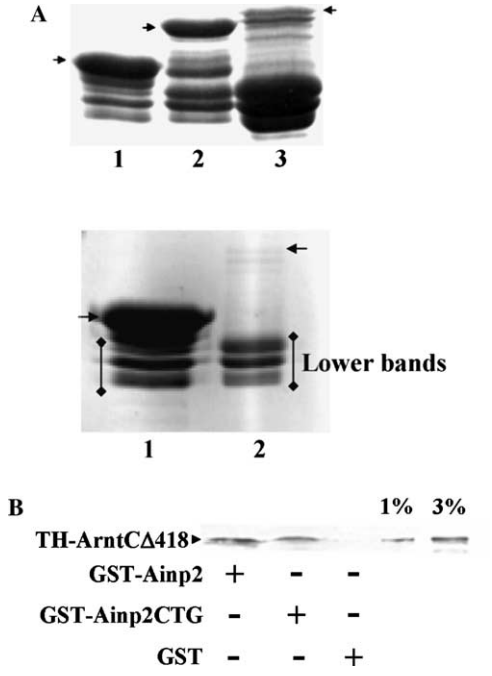


Fig. 4. GST pull-down assay showing Ainp2 interaction with TH-ArntCΔ418. (A) Coomassie blue staining of GST fusion proteins. Top: lane 1, GST; lane 2, GST-Ainp2; and lane 3, GST-Ainp2CTG. Bottom: lane 1, GST and lane 2, GST-Ainp2CTG. Samples were separated by 12% SDS–PAGE. Arrows indicate the recombinant proteins of interest. The sample amounts were adjusted on the bottom gel to show the presence of the lower bands in GST and GST-Ainp2CTG. (B) Western blot of GST pull-down assay showing interaction between TH-ArntCΔ418 and Ainp2. TH-ArntCΔ418 (100 μL) was used as the bait. Lane 1, 7.5 μg of GST-Ainp2; lane 2, 7.5 μg of GST-Ainp2CTG; lane 3, 7.5 μg of GST; lanes 4 and 5, percent of TH-ArntCΔ418 used for the assay (1 or 3%). The Anti-Thio antibody was used to detect TH-ArntCΔ418. The arrow indicates the TH-ArntCΔ418 protein. This experiment was repeated two more times with reproducible results.

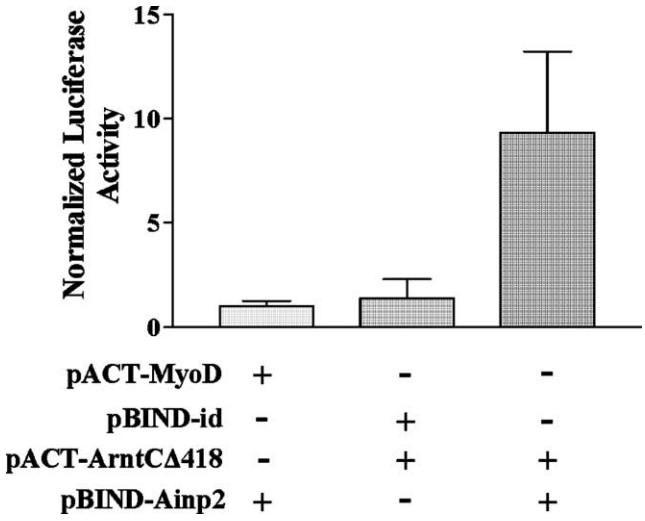


Fig. 5. Mammalian two-hybrid assay showing the Ainp2 interaction with TH-ArntCΔ418 in HepG2 cells. Plasmids transfected: lane 1, pACT-MyoD/pBIND-Ainp2; lane 2, pACT-ArntCΔ418/pBIND-id; and lane 3, pACT-ArntCΔ418/pBIND-Ainp2. The luciferase activities were normalized by the internal standard β-galactosidase activity. Activity of lane 1 was arbitrarily set to one. Data shown are the means ± SD, $n = 6$ (two independent experiments, each in triplicate).

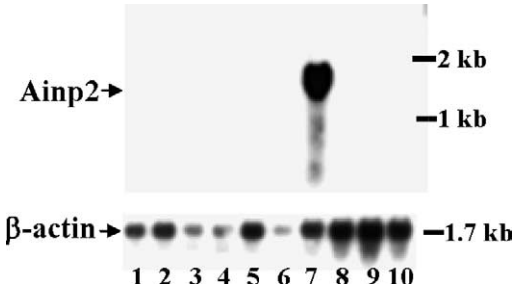


Fig. 6. Tissue specific expression of Ainp2. Northern blot analysis of Ainp2 using Ambion FirstChoice human pre-made blot. 1, brain; 2, placenta; 3, skeletal muscle; 4, heart; 5, kidney; 6, pancreas; 7, liver; 8, lung; 9, spleen; and 10, colon. Arrows indicate the Ainp2 transcript and the loading standard β-actin.

## Discussion

Phage display is a powerful technique to identify small peptides that interact with a protein. It is particularly useful for antibody characterization since the epitopes for antigen recognition are relatively small. Bacteriophage T7 is capable of displaying thousand copies of a small peptide (typically up to 50 amino acids [27]) on a phage particle, allowing efficient isolation of the interacting phages using a bait protein. In our case, we wanted to maximize the size of peptides displayed on the phage surface to optimize the expression of an Arnt-interacting domain. We used a human liver cDNA library cloned into 10-3B phage which allows expression of peptides that are up to 1000 amino acids in length in theory. Although only 5–15 peptides are expected to express on a phage surface using this phage, we observed a 100-fold enrichment of interacting phages (versus 15-fold using the negative control thioredoxin) after five rounds of biopanning, suggesting that the biopanning process was working properly. We intentionally used a thioredoxin-Arnt fusion (TH-ArntCΔ418) as the bait protein because (1) TH-ArntCΔ418 is expressed well in bacteria and is capable of dimerizing with AhRCΔ553 and forming the AhR/Arnt/DRE complex in the gel shift assay [26]; (2) thioredoxin can be conveniently used as the negative control; (3) TALON co-precipitation assay can be used as the biopanning protocol and (4) TH-ArntCΔ418 can be radiolabelled and then used as a probe for the secondary screening.

Membrane lift assay using $^{32}$P-labelled TH-ArntCΔ418 was performed to confirm that the amplified phages from biopanning did interact with the Arnt bait before further characterization (Fig. 2F). We focused on the longer pieces of isolated cDNA fragments (so that 200 bp fragments were intentionally excluded), with the hope that they would reveal longer pieces of an open

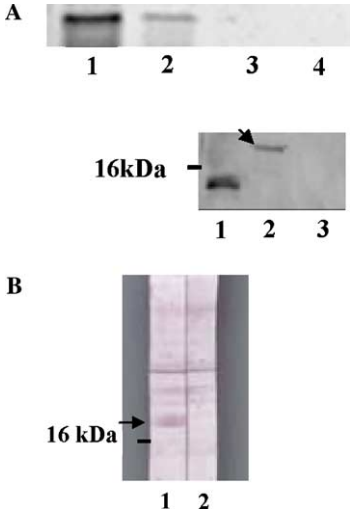


Fig. 7. Endogenous Ainp2 expression in Jurkat cells. (A) RT-PCR (upper) and Western blot (lower) showing the Ainp2 expression in Jurkat cells. RT-PCR (upper): A normalized amount of reverse transcription reaction mixture was used. The expected Ainp2 product (921 bp) is shown. Lane 1, Ambion RACE cDNA (positive control); lane 2, Jurkat; lane 3, HepG2; and lane 4, Hepa-1. Western (lower): lane 1, bacterially expressed His-Ainp2CTG (0.4 μL); lane 2, Jurkat soluble extract (40 μg); and lane 3, soluble extract from cryopreserved human hepatocytes (300 μg). The arrow (lane 2) indicates the Jurkat Ainp2 protein at ~20 kDa. Antiserum C634FB (1:500) was used as the primary antibodies. (B) 187.5 μL of Jurkat soluble extract was loaded on a one-lane 15% tricine SDS–PAGE gel. After transfer, the nitrocellulose membrane was cut into strips and incubated with the following primary antibodies: lane 1, C634FB (1:500) and lane 2, C634FB (1:500) pre-treated with 6His-Ainp2CTG and TALON resin. The arrow indicates the endogenous Ainp2 protein in Jurkat cells. This Western was repeated two more times ($n = 3$) to confirm the finding.

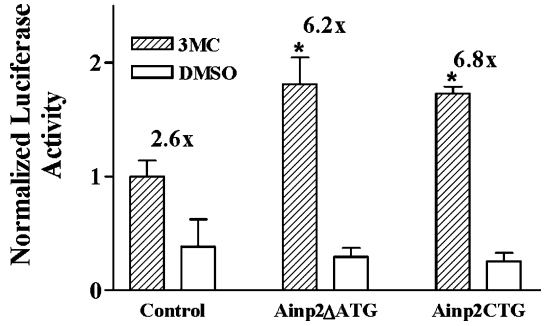


Fig. 8. Effect of Ainp2 on the 3MC-dependent induction of luciferase activity in HepG2 cells. In a 24-well plate, 0.33 μg each of empty pCMV-Tag4 vector (control, left), pCMV-Ainp2ΔATG vector (middle) or pCMV-Ainp2CTG vector (right) was transfected with pCH110 (0.33 μg) and pGudLuc1.1 plasmids. Each of the luciferase activity was normalized against the corresponding β-galactosidase activity. Fold induction by 3MC over the DMSO control was included (2.6-, 6.2-, and 6.8-fold for control, Ainp2ΔATG and Ainp2CTG, respectively). This experiment was done two times and each in triplicate ($n = 6$, means ± SD). The asterisks (*) indicate a statistically significant difference (two-tailed unpaired $t$ test, $p < 0.001$) of 3MC-treated Ainp2CTG or Ainp2ΔATG compared to the 3MC treated control.

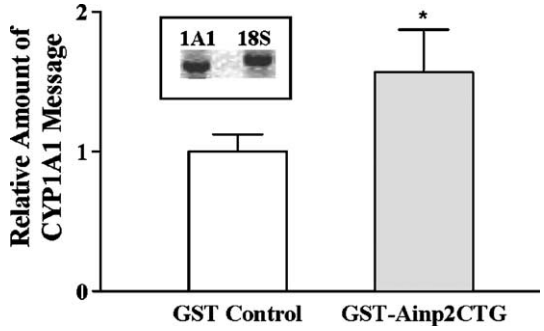


Fig. 9. Effects of Ainp2 on the CYP1A1 induction in HepG2 cells by 3MC. In a six-well plate, 3 μg of pCMV-GST (control) or pCMV-GST-Ainp2CTG was transfected. RT followed by real-time QPCR was performed to determine the CYP1A1 mRNA level. This experiment was repeated once for a total of five replicates ($n = 5$) of GST and six replicates ($n = 6$) of Ainp2CTG. The data represents mean ± SD of the amount of CYP1A1 gene normalized to the corresponding 18S. Agarose gel showing the PCR products of CYP1A1 (340 bp) and 18S (376 bp) was included. The asterisk (*) indicates a statistically significant difference between the GST control and Ainp2CTG (two-tailed unpaired $t$ test, $p < 0.005$).

reading frame. As a result, we have identified two peptides, Ainp1 and Ainp2, and both are 58 amino acids in length. We did not observe any interacting phage that contained the cDNA of a known Arnt-interacting protein such as AhR [28], HIF-1α [2], EPAS1 [29], AINT [30], SRC-1 [31], TRIP230 [32] or CoCoA [33]. We were not surprised because the minimal functional constructs of some of these proteins are known [AhR (aa 1–289) [34], HIF-1α (>aa 1–166) [35], SRC-1 (aa 763–1033) [31] and TRIP230 (aa 1583–1978) [32]] and they are larger than the phage peptides. As for CoCoA, our Arnt construct CΔ418 (aa 1–371) may not interact properly with CoCoA since it does not contain the whole PAS-B domain and is smaller than the Arnt construct (aa 1–458) used for the CoCoA interaction studies [33]. In addition, we would not expect to obtain an AINT-containing phage since the AINT mRNA was only found in mouse embryos whereas the adult liver cDNA library was used for our screening.

Results from GST pull-down assay, mammalian two-hybrid assay, and transient transfection studies examining the Ainp2 effect on the reporter gene expression and the endogenous CYP1A1 message unambiguously supported that Ainp2 interacts with Arnt and enhances the AhR signaling pathway. GST pull-down assay provided strong proof that Ainp2 interacts with Arnt in vitro; Arnt was clearly co-precipitated by either Ainp2 peptide or Ainp2CTG whereas the negative control GST did not precipitate Arnt (Fig. 4B). The results from the mammalian two-hybrid studies also confirmed that Ainp2 interacts with Arnt: almost 7-fold increase in the luciferase activity was caused by the Arnt–Ainp2 interaction, relative to the Arnt-id and MyoD-Ainp2 controls (Fig. 5). This interaction appears to play a role in the AhR signaling since expression of Ainp2 enhances the 3MC-dependent induction of the luciferase activity and of the CYP1A1 message in HepG2 cells. However, we found

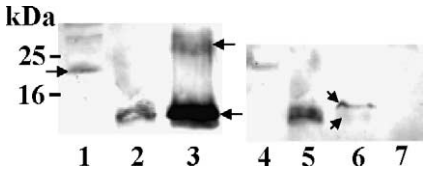


Fig. 10. Expression of 6His-Ainp2CTG in Sf9 and MCF7 cells. 6His-Ainp2CTG is expressed in Sf9 cells using a baculovirus system and in MCF7 cells by transient transfection. Lanes 1 and 4, Jurkat soluble extract (12.5 μL); lanes 2 and 5, bacterially expressed 6His-Ainp2CTG (0.4 μL); lane 3, baculovirus 6His-Ainp2CTG (10 μL); lane 6, MCF7 soluble extract transfected with pCMV-6His-Ainp2CTG (150 μg); and lane 7, wild type MCF7 soluble extract (150 μg). Arrow at lane 1 indicates Jurkat Ainp2. Arrows at lane 3 indicate 6His-Ainp2CTG with (upper) and without (lower) post-translational modification. Arrows at lane 6 indicate 6His-Ainp2CTG with (upper) and without (lower) post-translational modification. Proteins were resolved by a 15% tricine SDS–PAGE gel, followed by Western blot analysis using anti-Ainp2 antibodies C634FB (1:500).

that Ainp2 is not endogenously expressed in HepG2 cells, suggesting that Ainp2 is not important for the AhR signaling in HepG2 cells.

The putative full-length Ainp2 protein contains 77 amino acids with an estimated size of 9 kDa. We believe that we have obtained the full-length Ainp2 sequence because there are in-frame stop codons in the 5′ and 3′ UTR (Fig. 3). Although we did not see the starting methionine, we observed a possible start codon CUG (ANNCUGA) which contains a quasi Kozak sequence (adenine at −3 and guanine instead of adenine at +4 positions) [36]. A hairpin loop structure is present downstream to that CUG (+11 to +34) with 67% GC content; this fact supports the possibility that the 40S ribosome may stall and recognize the upstream CUG as the starting codon [36]. Additionally, 5′ RACE reaction was performed in two independent experiments, and in both cases we obtained the same sequence information with three in-frame stop codons upstream of the CTG, suggesting that a non-AUG start codon is likely. When we expressed the putative full-length Ainp2 cDNA with either its native CTG or an ATG at that location in HepG2 cells, both proteins enhanced the 3MC-induced luciferase activity to a similar extent, suggesting that the CUG is possibly the starting codon (Fig. 8).

Although our Northern blot analysis results showed that Ainp2 mRNA is predominantly found in human liver, we were not able to detect Ainp2 expression in three hepatoma cell lines (Hep3B, HepG2, and Hepa-1) and cryopreserved human hepatocytes (Fig. 7A and unpublished data). It appears that expression of Ainp2 is present in normal human liver and is sensitive to cell transformation (as in the case of cancer cell lines) and manipulation (as in the case of hepatocyte preparation). Since some EST clones from Jurkat cells contain the Ainp2 open reading frame, we searched for Ainp2 in Jurkat cells and found its expression at both the mRNA and protein levels. This endogenous Ainp2 protein appears to be larger than the bacterially expressed Ainp2CTG (20 versus 9 kDa). Certainly two obvious possibilities are that (1) we do not have the full-length Ainp2 and (2) Jurkat cells contain a splice variant of Ainp2. The size of the Ainp2 transcript from our Northern blot analysis (between 1000 and 2000 nucleotides) favors an Ainp2 protein that has a larger size than our putative full-length cDNA (1071 nucleotides). However, the Northern blot analysis was done using a small premade blot that the size should not be accurate. Additionally it is possible that Ainp2 has a long poly(A) tail in human liver that led to a longer transcript observed on the Northern blot. Another likely possibility for the size discrepancy is that Ainp2 is post-translationally modified in Jurkat cells since it contains numerous phosphorylation sites, and our bacterially expressed Ainp2CTG is not phosphorylated. To examine this possibility, we expressed 6His-Ainp2CTG in Sf9 and MCF7 cells. The expressed protein appears to be post-translationally modified; however, the modified 6His-Ainp2CTG and Jurkat Ainp2 are distinctly different in size (Fig. 10). It is important to note that the modified baculovirus 6His-Ainp2CTG is larger than the Jurkat Ainp2. Hence, it is possible that Ainp2CTG is the full-length protein and variation in protein sizes is caused by cell-specific post-translational modification.

From searching the GenBank database, we were unable to find the identity of Ainp2, suggesting that Ainp2 is a novel protein that has not been characterized. Nonetheless, there is much evidence supporting that Ainp2 is an endogenous protein: (1) Jurkat cells contain the Ainp2 mRNA and protein (Fig. 7); (2) results from the Northern blot analysis revealed that the Ainp2 mRNA is expressed and is predominantly found in human liver (Fig. 6); (3) since the Ambion cDNA library is generated primarily from mRNAs that contain the 5′ cap and the poly(A) tail, the Ainp2 mRNA must be present since we were able to obtain sequence information of Ainp2 from 3′ and 5′ RACE using this cDNA library; and (4) eight EST clones are found to contain the whole open reading frame of Ainp2.

The Ainp2 sequence contains neither the PAS nor the coiled coil sequences that are known to interact with Arnt. Although there is no known signature motif found on Ainp2, interestingly its sequence is serine/threonine-rich. Twenty-five percent of the Ainp2 sequence is serine or threonine and eleven potential phosphorylation sites are found on Ainp2 using the GeneTool software. Since there has been some evidence supporting that protein phosphorylation is involved in the signaling pathways of AhR [37,38], HIF-2α [39] and Arnt homodimer [40], it would be conceivable that protein phosphorylation or dephosphorylation of Ainp2 may be involved in the Arnt-dependent function. In addition, protein kinase C has been implicated to play a role in the AhR signaling pathway [41] and perhaps phosphorylation of Ainp2 by

protein kinase C is involved. Interestingly, a significant part of the cDNA sequence (77.6%) is the reverse complement to the haptoglobin cDNA, which is localized in human chromosome 16. We are currently investigating whether Ainp2 plays a role in regulating the haptoglobin message.

## Acknowledgments

We thank Dr. Mike Denison (UC, Davis) for providing the reporter plasmid pGudLuc1.1 and Dr. David Thomas (University of the Pacific) for providing Jurkat cells. This work is supported by a grant from the National Institute of Environmental Health Sciences (ES09794).

## Appendix A. Supplementary data

Supplementary data associated with this article can be found, in the online version, at doi:10.1016/j.abb.2005.06.026.

## References

[1] F.J. Gonzalez, P. Fernandez-Salguero, Drug Metab. Dispos. 26 (1998) 1194–1198.
[2] G.L. Wang, B.H. Jiang, E.A. Rue, G.L. Semenza, Proc. Natl. Acad. Sci. USA 92 (1995) 5510–5514.
[3] K. Kasuno, S. Takabuchi, K. Fukuda, S. Kizaka-Kondoh, J. Yodoi, T. Adachi, G.L. Semenza, K. Hirota, J. Biol. Chem. 279 (2004) 2550–2558.
[4] G.L. Semenza, Trends Mol. Med. 8 (2002) S62–S67.
[5] E. Maltepe, J.V. Schmidt, D. Baunoch, C.A. Bradfield, M.C. Simon, Nature 386 (1997) 403–407.
[6] A. Luzzago, F. Felici, A. Tramontano, A. Pessi, R. Cortese, Gene 128 (1993) 51–57.
[7] C.L. Jellis, T.J. Cradick, P. Rennert, P. Salinas, J. Boyd, T. Amiraault, G.S. Gray, Gene 137 (1993) 63–68.
[8] M. Bluthner, E.K. Bautz, F.A. Bautz, J. Immunol. Methods 198 (1996) 187–198.
[9] D. Blazek, V. Celer, I.I. Navratilova, P. Skladal, J. Virol. Methods 115 (2004) 83–92.
[10] R. Azriel-Rosenfeld, M. Valensi, I. Benhar, J. Mol. Biol. 335 (2004) 177–192.
[11] L. Riechmann, M. Weill, Biochemistry 32 (1993) 8848–8855.
[12] B. Stijlemans, K. Conrath, V. Cortez-Retamozo, H. Van Xong, L. Wyns, P. Senter, H. Revets, P. De Baetselier, S. Muyldermans, S. Magez, J. Biol. Chem. 3 (2003) 3.
[13] M.Y. Zhang, Y. Shu, S. Phogat, X. Xiao, F. Cham, P. Bouma, A. Choudhary, Y.R. Feng, I. Sanz, S. Rybak, C.C. Broder, G.V. Quinnan, T. Evans, D.S. Dimitrov, J. Immunol. Methods 283 (2003) 17–25.
[14] K. Manoutcharian, G. Acero, M.E. Munguia, J.A. Montero, T. Govezensky, C. Cao, K. Ugen, G. Gevorkian, J. Neuroimmunol. 145 (2003) 12–17.
[15] W.G. Willats, Plant Mol. Biol. 50 (2002) 837–854.
[16] C.L. Hsu, Y.L. Chen, S. Yeh, H.J. Ting, Y.C. Hu, H. Lin, X. Wang, C. Chang, J. Biol. Chem. 278 (2003) 23691–23698.
[17] D.A. Gearhart, P.F. Toole, J. Warren Beach, Neurosci. Res. 44 (2002) 255–265.
[18] M. Koolpe, M. Dail, E.B. Pasquale, J. Biol. Chem. 277 (2002) 46974–46979.
[19] C. Butteroni, M. De Felici, H.R. Scholer, M. Pesce, J. Mol. Biol. 304 (2000) 529–540.
[20] J.T. Lin, J.T. Lis, Mol. Cell. Biol. 19 (1999) 3237–3245.
[21] P. Wojnar, M. Lechner, P. Merschak, B. Redl, J. Biol. Chem. 276 (2001) 20206–20212.
[22] K. Hertveldt, M.L. Dechassa, J. Robben, G. Volckaert, Gene 307 (2003) 141–149.
[23] W.K. Chan, R. Chu, S. Jain, J.K. Reddy, C.A. Bradfield, J. Biol. Chem. 269 (1994) 26464–264671.
[24] P.V. Shetty, B.Y. Bhagwat, W.K. Chan, Biochem. Pharmacol. 65 (2003) 941–948.
[25] P.V. Shetty, X. Wang, W.K. Chan, Arch. Biochem. Biophys. 429 (2004) 42–49.
[26] A.B. Delucchi, K.A. Jensen, W.K. Chan, Biomol. Eng. 20 (2003) 1–5.
[27] Novagen, T7Select phage display system user manual.
[28] E.C. Hoffman, H. Reyes, F.F. Chu, F. Sander, L.H. Conley, B.A. Brooks, O. Hankinson, Science 252 (1991) 954–958.
[29] H. Tian, S.L. McKnight, D.W. Russell, Genes Dev. 11 (1997) 72–82.
[30] C.M. Sadek, S. Jalaguier, E.P. Feeney, M. Aitola, A.E. Damdimopoulos, M. Pelto-Huikko, J.A. Gustafsson, Mech. Dev. 97 (2000) 13–26.
[31] T.V. Beischlag, S. Wang, D.W. Rose, J. Torchia, S. Reisz-Porszasz, K. Muhammad, W.E. Nelson, M.R. Probst, M.G. Rosenfeld, O. Hankinson, Mol. Cell. Biol. 22 (2002) 4319–4333.
[32] T.V. Beischlag, R.T. Taylor, D.W. Rose, D. Yoon, Y. Chen, W.H. Lee, M.G. Rosenfeld, O. Hankinson, J. Biol. Chem. 279 (2004) 54620–54628 , Epub 2004 Oct 13..
[33] J.H. Kim, M.R. Stallcup, J. Biol. Chem. 279 (2004) 49842–49848.
[34] K.M. Dolwick, H.I. Swanson, C.A. Bradfield, Proc. Natl. Acad. Sci. USA 90 (1993) 8566–85670.
[35] B.H. Jiang, E. Rue, G.L. Wang, R. Roe, G.L. Semenza, J. Biol. Chem. 271 (1996) 17771–17778.
[36] M. Kozak, J. Biol. Chem. 266 (1991) 19867–19870.
[37] Y. Tian, S. Ke, M. Chen, T. Sheng, J. Biol. Chem. 278 (2003) 44041–44048.
[38] G.D. Minsavage, D.P. Vorojeikina, T.A. Gasiewicz, Arch. Biochem. Biophys. 412 (2003) 95–105.
[39] P.W. Conrad, T.L. Freeman, D. Beitner-Johnson, D.E. Millhorn, J. Biol. Chem. 274 (1999) 33709–33713.
[40] W.P. Long, X. Chen, G.H. Perdew, J. Biol. Chem. 274 (1999) 12391–12400.
[41] Y.H. Chen, R.H. Tukey, J. Biol. Chem. 271 (1996) 26261–26266.